Supporting Information

Tunable Photoluminescence and Enhanced Photoelectric Response of Mn^{2+}-Doped CsPbCl$_3$ Perovskite Nanocrystals via Pressure-Induced Structure Evolution

Junkai Zhang[a], Sihang Ji[b], Yanzhang Ma[c], Renquan Guan[a], Xiaoxin Wu[a], Xin Qu[a], Bingmin Yan[d,*], Dongzhou Zhang[e], Jialong Zhao[a,*], Jinghai Yang[a,*]

[a]Key Laboratory of Functional Materials Physics and Chemistry of the Ministry of Education, Jilin Normal University, Siping 136000, P. R. China

[b]Department of Physics, Jilin University, Changchun 130023, P. R. China

[c]Department of Mechanical Engineering, Texas Tech University, Lubbock, TX 79409, USA

[d]Center for High Pressure Science and Technology Advanced Research, Beijing 100094, P. R. China

[e]Hawai'i Institute of Geophysics and Planetology, School of Ocean and Earth Science and Technology, University of Hawai'i at Manoa, Honolulu, Hawaii 96822, USA

*To whom correspondence should be addressed. E-mail: bingmin.yan@hpstar.ac.cn (B. Yan), zhaojl@ciomp.ac.cn (J. Zhao) and jhyang1@jlnu.edu.cn (J. Yang).

Experimental details

Sample Preparation and Characterization.

Mn^{2+}:$CsPbCl_3$ NCs with a typical Mn^{2+}-doping concentration of 2.4% (relative to Pb^{2+}) were synthesized using an improved one-pot injection method. The $PbCl_2$ (0.2 mmol, 0.054 g) and $MnCl_2$ (0.4 mmol, 0.05 g) were mixed with OLA (1.5 mL), OA (1.5 mL), TOP (2 mL), and ODE (5 mL) in a 50 mL three-necked flask. The reaction mixture was degassed at 110 °C for 30 mins and then heated up to 190 °C under an argon flow. A 0.25 mL portion of Cs-oleate precursor (made by dissolving Cs_2CO_3, 0.22 g, in OA, 0.65 mL, and ODE, 10 mL, at 150 °C) was quickly injected into the reaction solution, and maintained for 1 min to allow the growth of Mn^{2+}-doped perovskite NCs, followed by immersing the flask in an ice water bath to quench the reaction. For purification, Mn^{2+}:$CsPbCl_3$ NCs were repeatedly precipitated by acetone/hexane, centrifuged, decanted, and suspended in hexane. The Mn^{2+} concentrations were monitored by inductively coupled plasma-mass spectrometry (ICP-MS) after each purification cycle to ensure elimination of all unincorporated Mn^{2+}, and the process was repeated until the Mn^{2+} concentrations became independent of further purification cycles, typically after 3 or 4 cycles. Absorption spectra were recorded on a UV-vis spectrophotometer (Shimadzu UV-2700). PL excitation spectra and PL decay curves were carried out using a spectrometer (Horiba Jobin Yvon Fluorolog-3) with a time-correlated single-photon counting lifetime spectroscopy system. The crystal structure and microstructural morphologies of the sample were measured at ambient pressure, using XRD with λ= 1.5418 Å from the CuKα radiation (Rigaku D/max-2500) and TEM (JEOL 2100). A PerkinElmer Nexion350-X inductively coupled plasma-mass spectrometer (ICP-MS) was used for elemental analysis. The structural optimization, bond length and density of state for $CsPbCl_3$ and Mn^{2+}:$CsPbCl_3$ were performed in the framework of density functional theory (DFT) using the Vienna ab initio simulation package (VASP) [S1] with a 2 × 2 supercell. The projector-augmented plane wave (PAW) [S2] approach was used to represent the ion-electron interaction. The electron exchange-correlation functional was treated using the generalized gradient approximation (GGA) proposed by Perdew, Burke and Ernzerhof (PBE) [S3]. The energy cutoff of the plane wave was set to be 360 eV with the energy precision of 10^{-4} eV. The Brillouin zone was sampled with a 2 × 2 × 2 Γ-centered Monkhorst-Pack k-point grid for geometry optimization and self-consistent calculations.

High-Pressure Generation.

A symmetrical diamond anvil cell (DAC) with a pair of diamond anvils with 400 μm culets was employed to generate high pressure. A T301 steel gasket was pre-indented to 40 μm in thickness, and a hole with a 150 μm diameter was drilled at the center of the dent as the sample chamber for high-pressure absorption, PL, and XRD measurements. The powder sample and a small ruby ball were placed into the sample chamber, and the *in situ* pressure was gauged by the R_1 ruby fluorescence shift. Silicon oil was used as the pressure-transmitting medium. The schematic drawing of the sample assembly is clearly shown in Figure S1. A nonmagnetic rhenium sheet, used as another gasket, was pre-indented to 50 μm in thickness. A hole with 200 μm in diameter was drilled at the center of the indentation using a laser. Then, a mixture of alumina powder and epoxy was inserted and compressed into the hole as the insulating layer. Subsequently, another hole with 150 μm was drilled and served as the sample chamber for high-pressure impedance spectra and photocurrent measurements. The thickness of the sample under high pressure was determined using a micrometer with a precision of 0.5 μm. No pressure medium was loaded in order to avoid additional errors in electrical measurements. The ruby fluorescence method was also used for the pressure calibration.

***In situ* High-Pressure Absorption and PL Measurements.**

High-pressure absorption spectra were conducted using an Ocean Optics QE65000 scientific-grade UV-vis spectrophotometer. PL spectra were collected with Renishaw InVia spectrometer using a 325 nm continuous wave laser with an output power of 10 mW and a 50 times Leica optical microscope.

***In situ* High-Pressure Angle-dispersive XRD Measurements.**

High-pressure XRD experiments were conducted at the 13-BM-C station of the Advanced Photon Source (APS), Argonne National Laboratory (ANL) (λ=0.406750 Å). The experimental parameters, including the distance between sample and detector, were calibrated using conventional CeO_2 materials. Two-dimensional XRD images were induced into the format of intensity versus the diffraction angle (2θ), through integration via the FIT2D program.

***In situ* High-Pressure Impedance Spectra and Photocurrent Measurements**.

Parallel-plate capacitor electrodes and *Van der Pauw* configuration electrodes were integrated on the diamond culets for *in situ* high-pressure impedance spectra and photocurrent

measurements, respectively (Figure S2). The fabricated details of the different microcircuit probes on the diamond have been reported previously [S4,S5]. The impedance spectrum was obtained using a computer-controlled impedance analyzer (Solartron 1260), combined with a dielectric interface (Solartron 1296). A voltage signal with amplitude of 2 V, and frequency ranging from 10^{-2} to 10^{7} Hz was applied to the sample. The photocurrent was recorded by a CHI-760E electrochemical workstation. The illumination was simulated sunlight provided by a 500 W Xe lamp. The constant DC voltage of 5 V was applied to the sample. The interval time Δt between the light on and off was 20 s.
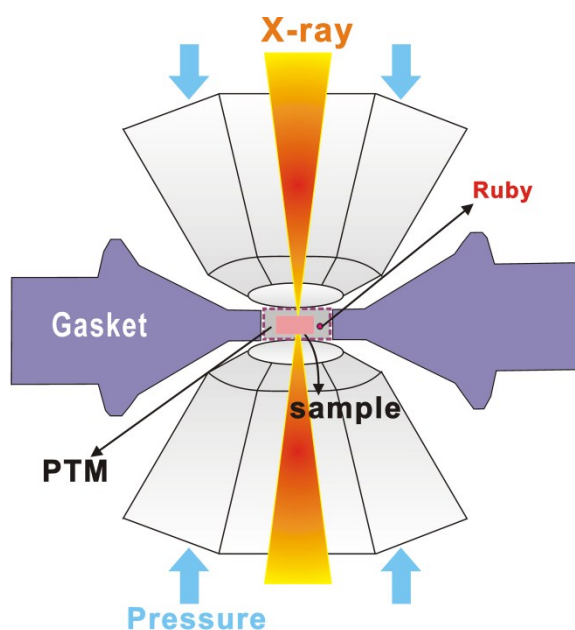
Figure S1. Schematic drawing of a symmetric DAC used in the high-pressure angle-dispersive XRD measurements.
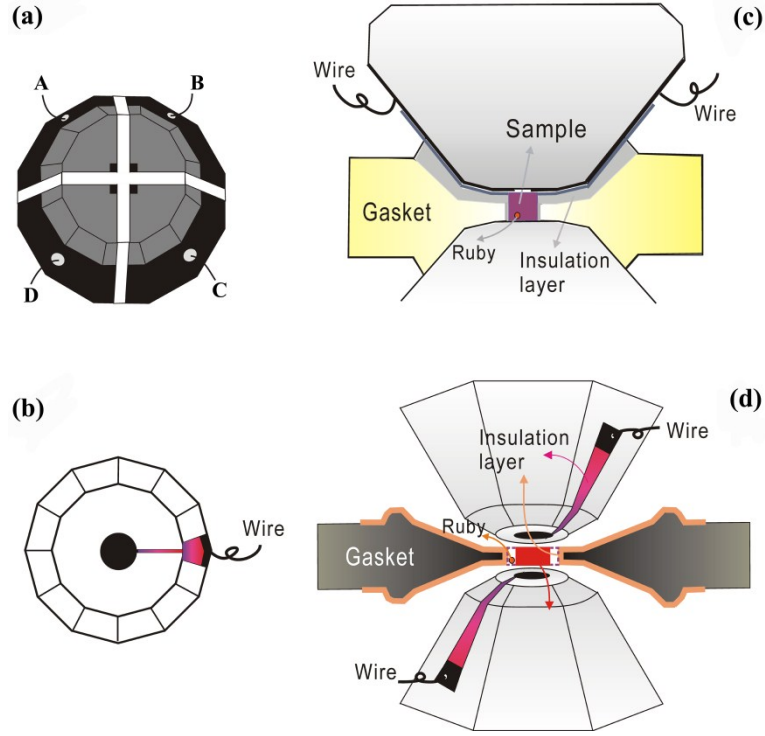
Figure S2. Configurations of the *Van der Pauw* microcircuit (a) and the parallel-plate capacitor electrodes (b) on a diamond anvil, respectively. (c) and (d) show the corresponding cross sections of the designed DAC to (a) and (b) respectively.

Figure S2 illustrates the configurations of the microcircuits using the *Van der Pauw* model and the parallel-plate capacitor electrodes, respectively, and the corresponding schematic views of the experimental setups can be found in [S6,S7].

Van der Pauw method utilizes the principle of the bridge circuit for resistance measurements and can successfully avoid contact and lead-wire resistance in measuring the resistance of samples in DAC [S8]. In this study, we adopted *Van der Pauw* electrodes with current reversal method to study the electrical properties, by which the following effects can be excluded, *i.e.* contact effect, heating effect of current and asymmetric effect of probing electrodes, *etc* [S6,S9]. In the resistivity measurements, a 10 mA (named I_1) direct current was first applied from A to B (as shown in Figure S2(a)), and the voltage drop (V_1) between C and D was recorded. Then, the same current (I_2) was applied from A to D, and the voltage drop (V_2) between B and C was recorded. The electrical resistivity was determined by the *Van der Pauw* equation: $\exp(-\pi L R_A/\rho_S) + \exp(-\pi L R_B/\rho_S) = 1$, where R_A and R_B are the measured resistances ($R_A = V_1/I_1$, $R_B = V_2/I_2$), L is the thickness of sample, and ρ_S is the electrical resistivity. The thickness of the sample under pressure was determined according to the measurement of changes in the distance between the back facets of the two anvils

with a modified micrometer having two symmetrical microprobes. By knowing the initial sample thickness, the thickness at pressures can be calculated accordingly [S10].

The impedance spectrum (IS) method is also available for *in-situ* analysis of materials under extreme conditions and can reveal many important properties such as conductivity, interface density, as well as dielectric characteristics [S11,S12]. During IS measurements, the major experimental problem is the poor contact between the electrode and the sample. The parallel-plate capacitor electrodes have fixed positions and well controlled shape in DAC, which can increase the contact area between the electrode and sample to the utmost extent, as a result effectively preventing the parasitic inductances from the chamber wall and the wire [S7]. In IS experiments, a small ac voltage signal should be introduced into the system being studied, the response of the system to this signal is always expressed by complex impedance $Z=Z'+iZ''$, where Z' and Z'' are the real part and imaginary part of Z. They change as a function of the signal frequency and related parameters of the system. If Z (or Z' and Z'') is determined, the characteristics of the system can be known.
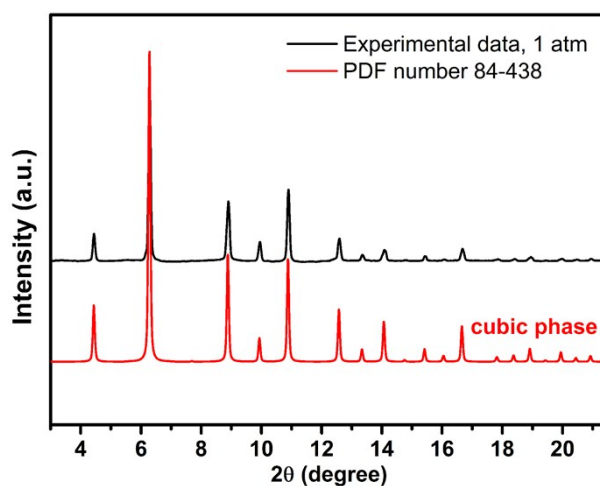

Figure S3. XRD patterns of as-synthesized Mn^{2+}:$CsPbCl_3$ NCs.

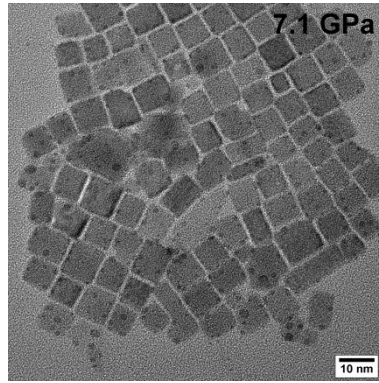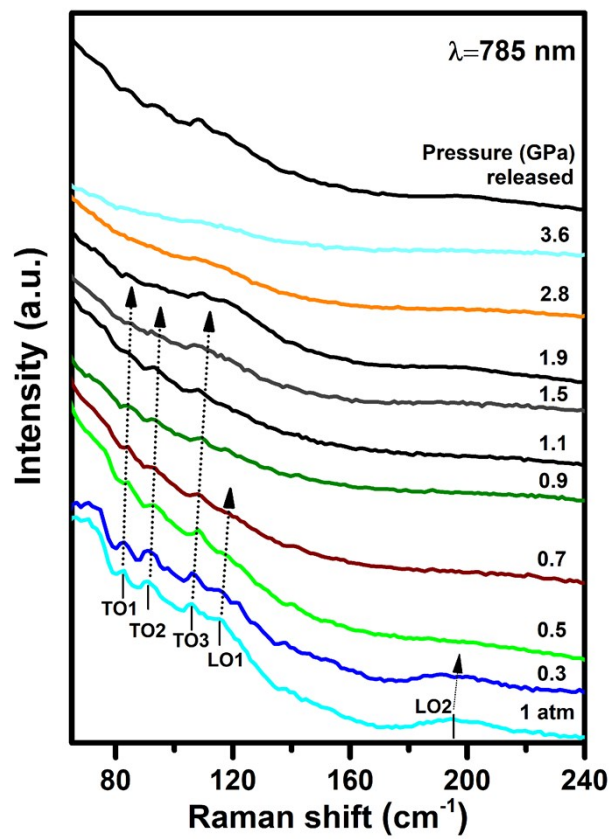Figure S4. TEM image of Mn^{2+}:CsPbCl$_3$ NCs quenched from 7.1 GPa in the *in-situ* high-pressure XRD measurements.

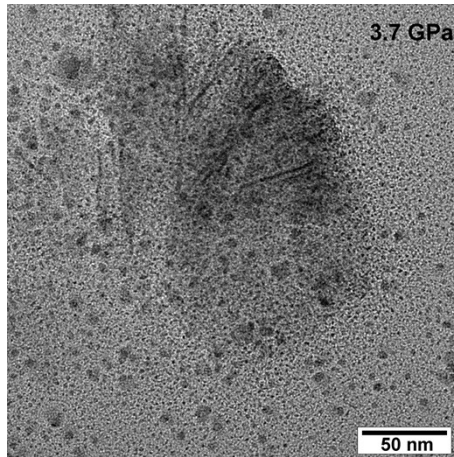Figure S5. Raman spectra of as-synthesized Mn^{2+}:CsPbCl$_3$ NCs under 785 nm excitation at selected pressures.

Figure S6. TEM image of thermally-annealed Mn^{2+}:$CsPbCl_3$ NCs quenched from 3.7 GPa in the *in-situ* high-pressure impedance spectra measurements.
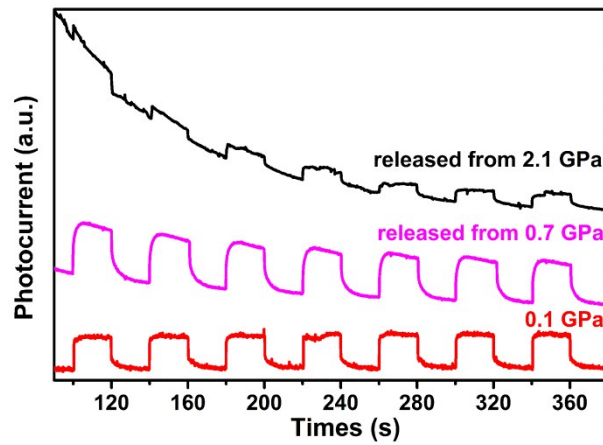

Figure S7. (a) Time-dependent photocurrent of thermally-annealed Mn^{2+}:$CsPbCl_3$ NCs at 0.1 GPa (red line) during compression and after pressure is fully released from 0.7 GPa (magenta line) and 2.1 GPa (black line), respectively.
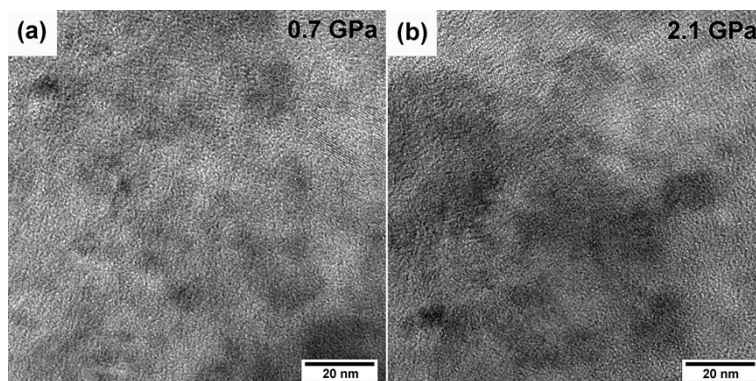

Figure S8. High-resolution TEM images of thermally-annealed Mn^{2+}:$CsPbCl_3$ NCs quenched from selected pressures: 0.7 GPa (a) and 2.1 GPa (b), respectively, in the *in-situ* high-pressure photocurrent measurements.

References

[S1] Kresse, G.; Furthmüller, J.; Efficient Iterative Schemes for ab Initio Total-Energy Calculations using a Plane-Wave Basis Set. *Phys. Rev. B* **1996**, *54*, 11169-11186.

[S2] Kresse, G.; Joubert, D.; From Ultrasoft Pseudopotentials to the Projector Augmented-Wave Method. *Phys. Rev. B* **1999**, *59*, 1758-1775.

[S3] Perdew, J. P.; Burke, K.; Ernzerhof, M.; Generalized Gradient Approximation Made Simple. *Phys. Rev. Lett.* **1996**, 77, 3865-3868.

[S4] Gao, C.; Han, Y.; Ma, Y.; White, A.; Liu, H.; Luo, J.; Li, M.; He, C.; Hao, A.; Huang, X. Accurate Measurements of High Pressure Resistivity in a Diamond Anvil Cell. *Rev. Sci. Instrum.* **2005**, *76*, 083912.

[S5] Wang, Q. L.; Liu, C. L.; Han, Y. H.; Gao, C. X.; Ma, Y. Z. The Determination of Ionic Transport Properties at High Pressures in a Diamond Anvil Cell. *Rev. Sci. Instrum.* **2016**, *87*, 123904.

[S6] Gao C.; Han Y.; Ma Y.; White A.; Liu H.; Luo J.; Li M.; He C.; Hao A.; Huang X. Accurate Measurements of High Pressure Resistivity in a Diamond Anvil Cell. *Rev. Sci. Instrum.* **2005**, *76*, 083912-1-4.

[S7] Wang Y.; Han Y. H.; Gao C. X.; Ma Y. Z.; Liu C. L.; Peng G.; Wu B. J.; Liu B.; Hu T. J.; Cui X. Y.; Ren W. B.; Li Y.; Su N. N.; Liu H. W.; Zou G. T. In situ Impedance Measurements in Diamond Anvil Cell under High Pressure. *Rev. Sci. Instrum*. **2010**, *81*, 013904-1-4.

[S8] Mao H. K.; Bell P. M. Electrical Resistivity Measurements of Conductors in the Diamond-Window, High-Pressure cell. *Rev. Sci. Instrum*. **1981**, *52*, 615-616.

[S9] Han Y. H.; Gao C. X.; Ma Y. Z.; Liu H. W.; Pan Y. W.; Luo J. F.; Li M.; He C. Y.; Huang X. W.; Zou G. T.; Integrated Microcircuit on a Diamond Anvil for High-Pressure Electrical Resistivity Measurement. *Appl. Phys. Lett.* **2005**, *86*, 0641042005-1-3.

[S10] Li M.; Gao C. X; Peng G.; He C. Y.; Hao A. M.; Huang X. W.; Zhang D. M.; Yu C. L.; Ma Y. Z.; Zou G. T. Thickness Measurement of Sample in Diamond Anvil Cell. *Rev. Sci. Instrum*. **2007**, *78*, 075106-1-3.

[S11] Knight J.; Nur A. The Dielectric Constant of Sandstones, 60 kHz to 4 MHz. *Geophysics* **1987**, *52*, 644-654.

[S12] Roberts J. J.; Tyburczy J. A. Impedance Spectroscopy of Single and Polycrystalline Olivine:

Evidence for Grain Boundary Transport. *Phys. Chem. Miner*. **1993**, *20*, 19-26.